Compatibility of FeCrAlMo in Flowing Pb-Li at 600°-700°C

B. A. Pint[1], J. Jun[1], E. Cakmak[1],
[1]Materials Science and Technology Division, Oak Ridge National Laboratory, Oak Ridge, TN
(pintba@ornl.gov, 865-576-2897)

D. J. Sprouster[2], N. Olynik[2] and L. L. Snead[2]
[2]Department of Material Science and Engineering, Stony Brook University, Stony Brook, NY

TOFE abstract number: FST19-230

ABSTRACT

A series of monometallic thermal convection loops (TCLs) has been conducted to determine the maximum temperature where FeCrAl alloys have compatibility with eutectic lead lithium (Pb-Li) for a dual coolant fusion blanket. Pre-oxidizing commercial alloy APMT (Fe-21Cr-5Al-3Mo) for 2h at 1000°C to form a surface α-Al_2O_3 layer was very effective in reducing the mass loss of specimens in the hot and cold legs of the most recent TCL that was operated for 1000 h with a peak temperature of 700°C. However, unlike previous experiments, the post exposure room temperature ductility of most of the APMT specimens was degraded to <10% total elongation and many of the specimens at the highest temperature (>680°C) were severely damaged or were not recovered. Wide angle x-ray scattering found that the preformed α-Al_2O_3 scale transformed to a mixture of trigonal and tetragonal $LiAlO_2$. The overall results suggest that the maximum temperature for FeCrAl is limited to <700°C.

Keywords: PbLi compatibility, FeCrAl, Al_2O_3, DCLL blanket

INTRODUCTION

To improve the efficiency of fusion energy, higher blanket temperatures are desired. However, increasing the operating temperatures can lead to compatibility issues with the coolant, particularly for Pb-Li in the dual coolant lead lithium (DCLL) blanket concept [1,2]. Forming a stable surface oxide or scale, like α-Al_2O_3[3] on an FeCrAl alloy or Al-rich coating [4,5], can inhibit dissolution compared to uncoated reduced activation ferritic-martensitic (RAFM) structural steels, which are limited to ~475°C in Pb-Li [6]. To determine the maximum temperature where this concept is effective, a series of monometallic thermal convection loops (TCLs) [7,8] have been fabricated from Kanthal alloy APMT (Fe-21Cr-5Al-3Mo) to test compatibility in flowing Pb-Li, where the temperature gradient enables continuous mass transfer [9,10]. This paper reports the results from APMT specimens exposed for 1000 h in the 4th TCL experiment with a peak temperature of 700°C. In addition, wide angle x-ray scattering (WAXS) [11] was used to study the formation of $LiAlO_2$ on bare and pre-oxidized APMT [8].

EXPERIMENTAL PROCEDURE

The TCL experiment followed a similar procedure as has been detailed elsewhere [7,8]. Specimen chains of 20 APMT (Fe-21.6wt%Cr-4.9%Al-2.8Mo-0.53Si-0.1Mn-0.1Ni-0.2Hf-0.1Y9.1Zr-0.03C) coupons (15 x 25 x 1 mm) and dogbone SS-3 type tensile specimens (25.4 mm long, 0.76 x 5 mm gage) were joined by 1mm diameter APMT wire and hung in the TCL hot leg (HL) and cold leg (CL). Most of the specimens were pre-oxidized for 2 h at 1000°C in laboratory air [8] and W spacers at the bottom of each chain prevented the chain from floating. The APMT loop tubing (26.7 mm diameter, 3.1 mm wall thickness) was pre-oxidized for 8 h at 1050°C as part of the post-weld heat treatment procedure [7] and a new loop was used for each TCL experiment. The commercial Pb-17at.%Li (0.68 ± 0.01 wt.%Li, ~1200 wppm O and ~240 wppm C [7]) was melted in a SS fill tank. Six thermowells at the top, middle and bottom of each leg were used to estimate each specimen temperature and the peak temperature of 700±1°C was controlled at the top of the HL. The temperature gradient was ~85°C and hot spot tests [7] measured a Pb-Li velocity of ~1.4 cm/s.

After the 1000 h exposure, the PbLi was dumped into a stainless steel tank and the TCL was cleaned using the standard solution of acetic acid, ethanol and hydrogen peroxide [7,8]. After disassembling, it was discovered that the second specimen in the hot leg chain had broken and 3 other specimens were missing and not found in the dump tank. The broken fracture suggested that the chain broke after the Pb-Li was dumped but could have occurred during the experiment. Specimens were weighed before and after exposure using a Mettler Toledo X205 balance. The coupons were analyzed using conventional x-ray diffraction (XRD) using a Malvern PANalytical X'Pert PRO diffractometer with CuKα radiation and two tensile specimens were examined using WAXS [11] at the National Synchrotron Light Source-II, using 15.1 keV X-rays and the background scattering patterns were subtracted to isolate the signal from the exposed surface and within the bulk (~100μm deep). Polished specimen cross-sections were characterized using light microscopy and scanning electron microscopy (Tescan MIRA3) equipped with energy dispersive X-ray spectroscopy (EDS). Post-exposure room temperature tensile testing was performed with a strain rate of 0.015/min per ASTM E8-13.

RESULTS AND DISCUSSION

The mass change data are shown in Figure 1. The first specimen in the hot leg showed a much larger mass loss than expected and no data were obtained for the next 4 specimens as noted above. The APMT wire used to connect the specimens may have been the weak link. Typical of prior APMT TCL experiments [7,8], the mass losses were higher for the APMT specimens that were not pre-oxidized and, for the pre-oxidized specimens, small mass losses were consistently observed. Figure 2 summarizes the mass loss data from all 4 monometallic TCL experiments [7,8]. The median mass loss values increased slightly with temperature in the cold leg but the change is not statistically significant and was not observed in the hot leg. Figure 2 indicates the mass losses for the specimens at 678° and 699°C shown in Figure 1 were higher than most other specimens. The temperatures in the TCL experiment are well over 550°C where dissolution of RAFM steel plugged flow in a pumped Pb-Li loop [6] due to mass transfer (i.e. dissolution and precipitation).

Figure 3 shows polished sections of bare and pre-oxidized APMT specimens from the hot and cold legs with the mass losses noted. In some cases the copper plating has separated from the specimens making it hard to assess the thickness of the surface oxide layer. The wavy or pitted interface regions suggest dissolution especially on the specimens with large mass losses. For the specimens that were not pre-oxidized, dissolution could have proceeded before an oxide layer was established. In some regions on the pre-oxidized specimens, the interface was flat, suggesting the pre-formed oxide had inhibited dissolution. Figure 4 shows SEM/EDS maps where a surface oxide layer could not be clearly identified for coupon specimens exposed in the hot leg (Figures 4a and 4d) and a cold leg coupon where the oxide was observed (Figure 4h). Using conventional XRD, the surface layers were identified by XRD as either γ-$LiAlO_2$ (tetragonal) for the bare APMT coupons or α-$LiAO_2$ (trigonal) for the pre-oxidized coupons. Those results are not shown here as they are similar to observations reported for the previous TCL experiment with a peak temperature of 650°C [8]. Coupon specimens were inserted to allow easier XRD characterization compared to the smaller tensile specimens.

To characterize the oxide scale on the smaller tensile specimens exposed in the hottest section, WAXS was employed. Figure 5 shows the results for the broken bare APMT specimen exposed at 696°C and a pre-oxidized specimens exposed at 681°C (-0.2 mg/cm^2 mass loss). Using this higher resolution technique, both α and γ $LiAlO_2$ phases were detected in the pre-oxidized specimen with none of the original α-Al_2O_3 detected. Previously, it was suggested that the mass losses in Figure 2 could be related to this phase transformation or slow continuous dissolution of the $LiAlO_2$ layer [8]. For the bare specimen, no clear peaks were detected. It is possible that the oxide was damaged during cleaning.

Figure 6 shows the post-exposure room temperature 0.2% yield stress and total elongation compared to those in the previous TCL experiment where the peak temperature was only 650°C (open symbols) [8]. In the previous TCL, only minor changes in tensile properties were noted after exposure compared to the as-received APMT tensile properties shown as the shaded areas in Figure 6. In the 700°C

TCL experiment, there was more variability in the post-exposure results and, in particular, a larger drop in ductility for some specimens, Figure 6b. At <500°C in the first TCL experiment, specimens were significantly embrittled by the formation of α′, which was identified by transmission electron microscopy [7]. At shown in Figure 6b, significant embrittlement was not observed from 530°-650°C in the previous TCL experiment and would not be expected at 650°-700°C. Also, the <500°C embrittlement was accompanied by a large increase in yield stress which was not observed for these specimens in Figure 6a.

In general, the larger mass losses in the hot leg of this experiment including the likely heavily attacked missing specimens (no specimens have been lost in previous TCL experiments at lower temperatures), leads to the conclusion that a surface oxide on APMT is not able to substantially reduce dissolution and mass transfer in flowing Pb-Li. Therefore, the maximum temperature appears to be ~650°C and future studies will focus on lower Pb-Li temperatures.

SUMMARY

To continue to explore the high temperature compatibility of FeCrAl in flowing Pb-Li, a 4th monometallic thermal convection loop (TCL) was run for 1000 h with a peak temperature of 700°C. Pre-oxidation for 2h at 1000°C to form an alumina layer prior to Pb-Li exposure reduced the mass losses in both the hot and cold legs of the loop. However, at the highest temperatures above 680°C, the APMT specimens were either not recovered or exhibited high mass losses. Also, the room temperature tensile properties were degraded with the majority of specimens showing <10% ductility after exposure, unlike the previous TCL with a peak temperature of 650°C. These results suggest that the upper temperature limit for alumina to protect FeCrAl from dissolution in PbLi may be below 700°C.

Acknowledgments

The experimental work was conducted by A. Willoughby, M. Stephens, B. Johnston, V. Cox and T. Lowe. M. Romedenne provided useful comments on the manuscript. This research was funded by the U.S. Department of Energy's Office of Fusion Energy Sciences.

References

1. S. MALANG, M. TILLACK, C. P. C. WONG, N. MORLEY and S. SMOLENTSEV, "Development of the Lead Lithium (DCLL) Blanket Concept," *Fusion Science and Technology*, **60**, *1*, 249 (2011).
2. M. ABDOU, N. B. MORLEY, S. SMOLENTSEV, A. YING, S. MALANG, A. ROWCLIFFE and M. ULRICKSON, "Blanket/first wall challenges and required R&D on the pathway to DEMO," *Fusion Engineering and Design*, **100**, 2 (2015).
3. P. HUBBERSTEY, T. SAMPLE and A. TERLAIN, "The Stability of Tritium Permeation Barriers and the Self-Healing Capability of Aluminide Coatings in Liquid Pb-17Li," *Fusion Technology*, **28**, 1194 (1995).
4. H. GLASBRENNER, J. KONYS, Z. VOSS and O. WEDEMEYER, "Corrosion behaviour of Al based tritium permeation barriers in flowing Pb–17Li," *Journal of Nuclear Materials* **307-311**, 1360 (2002).
5. S.-E. WULF, W. KRAUSS and J. KONYS, "Impact of pretreatment conditions on defect formation during the fabrication of Al-based corrosion barriers by ECX process," *Fusion Engineering and Design* **124**, 1091 (2017).
6. J. KONYS, W. KRAUSS, J. NOVOTNY, H. STEINER, Z. VOSS and O. WEDEMEYER, "Compatibility behavior of EUROFER steel in flowing Pb–17Li," *Journal of Nuclear Materials*, **386-388**, 678 (2009).
7. S. J. PAWEL and K. A. UNOCIC, Compatibility of an FeCrAl alloy with flowing Pb-Li in a thermal convection loop. *Journal of Nuclear Materials*, **492**, 41 (2017).
8. J. JUN, K. A. UNOCIC, M. J. LANCE, H. M. MEYER and B. A. PINT, "Compatibility of Alumina-Forming Steel with Flowing PbLi at 500°-650°C," *Journal of Nuclear Materials*, **528**, 151 (2020).
9. J. H. DEVAN, "Compatibility of Structural Materials with Fusion Reactor Coolant and Breeder Fluids," *Journal of Nuclear Materials*, **85-86**, 249 (1979).
10. P. F. TORTORELLI, "Dissolution Kinetics of Steel Exposed in Lead-Lithium and Lithium Environments," *Journal of Nuclear Materials*, **191-194**, 965 (1992).
11. D. J. SPROUSTER, J. R. TRELEWICZ, L. L. SNEAD, X. HU, D. MORRALL, T. KOYANAGI, C. M. PARISH, L. TAN, Y. KATOH and B. D. WIRTH, "Advanced synchrotron characterization techniques for fusion materials science," *Journal of Nuclear Materials*, **543**, 152574 (2021).

Figure Captions

Figure 1. Specimen mass change of APMT specimens as a function of estimated temperature in the hot leg (HL) and cold leg (CL) of the 700°C TCL experiment. The specimens without pre-oxidation are shown as open symbols.

Figure 2. Median mass change values for pre-oxidized APMT specimens in all four TCL experiments. The boxes show the 1st and 3rd quartiles and the whiskers the minimum and maximum values.

Figure 3. Light microscopy of representative APMT tensile specimens from the 700°C TCL experiment hot leg (HL) and cold leg (CL). A protective Cu layer was deposited before mounting.

Figure 4. (a,d,g) SEM secondary electron images of APMT exposed to PbLi for 1000 h and associated (b,e,h) Al and (c,f,i) O EDX maps.

Figure 5. WAXS spectra from two APMT specimens exposed at 681°C (16380) and 696°C (16375) with several identified and unidentified (circled) peaks. The data are plotted on a log scale to highlight the weak peak intensities. The 16375 spectra has negative peaks because the bulk intensities were subtracted from the surface pattern.

Figure 6. Post-exposure room-temperature tensile properties of APMT specimens as a function of estimated exposure temperature (a) yield stress and (b) total elongation. The open symbols are from the 650°C TCL and the closed symbols from the 700°C TCL. The baseline (as-received) properties are shown as a shaded band in each case.

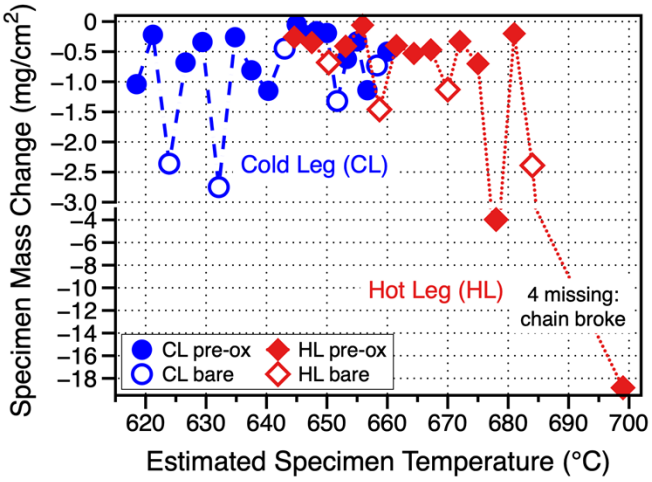

Figure 1. Specimen mass change of APMT specimens as a function of estimated temperature in the hot leg (HL) and cold leg (CL) of the 700°C TCL experiment. The specimens without pre-oxidation are shown as open symbols.

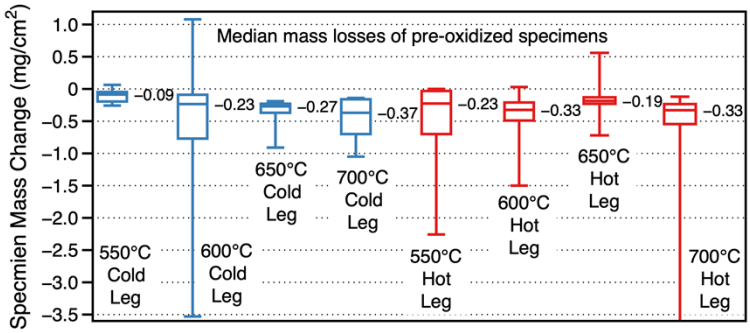

Figure 2. Median mass change values for pre-oxidized APMT specimens in all four TCL experiments. The boxes show the 1st and 3rd quartiles and the whiskers the minimum and maximum values.

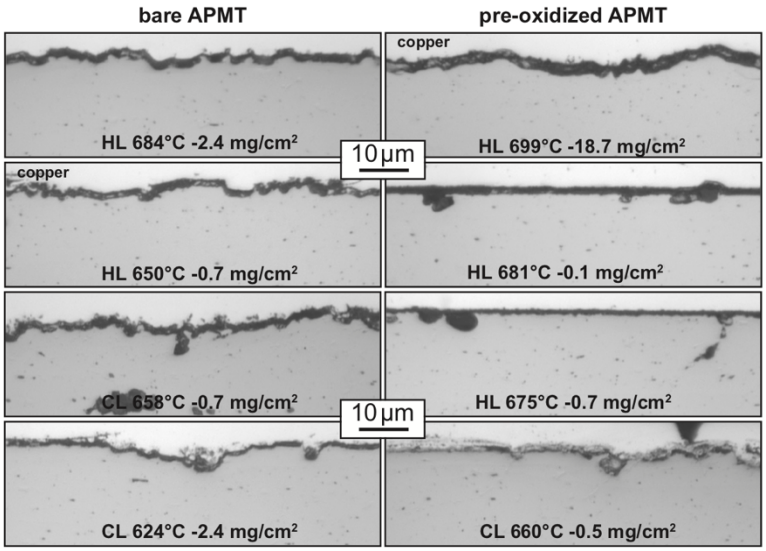

Figure 3. Light microscopy of representative APMT tensile specimens from the 700°C TCL experiment hot leg (HL) and cold leg (CL). A protective Cu layer was deposited before mounting.

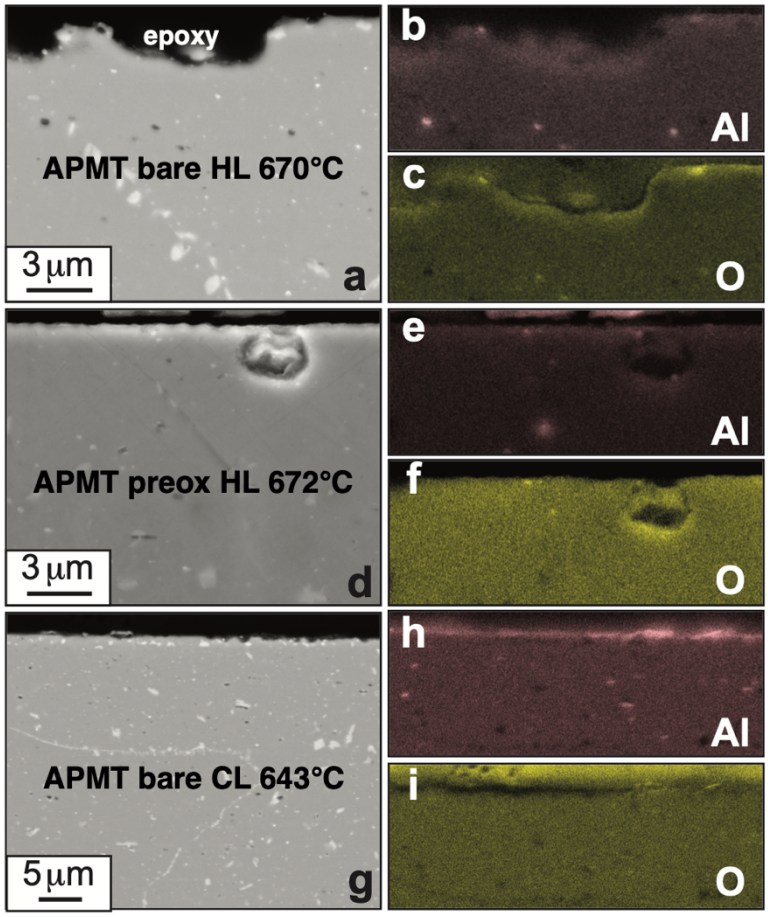

Figure 4. (a,d,g) SEM secondary electron images of APMT exposed to PbLi for 1000 h and associated (b,e,h) Al and (c,f,i) O EDX maps.

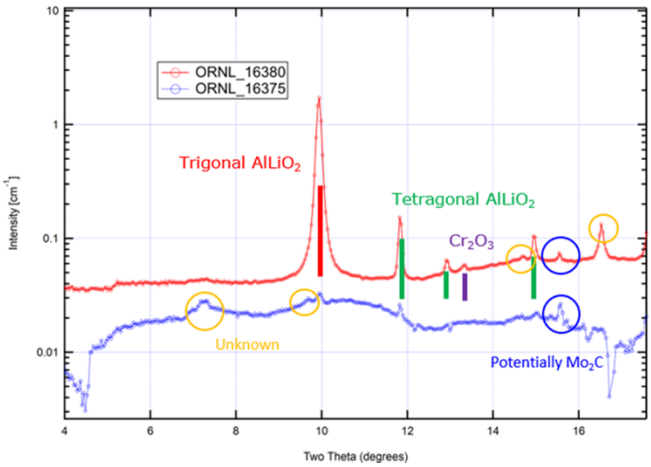

Figure 5. WAXS spectra from two APMT specimens exposed at 681°C (16380) and 696°C (16375) with several identified and unidentified (circled) peaks. The data are plotted on a log scale to highlight the weak peak intensities. The 16375 spectra has negative peaks because the bulk intensities were subtracted from the surface pattern.

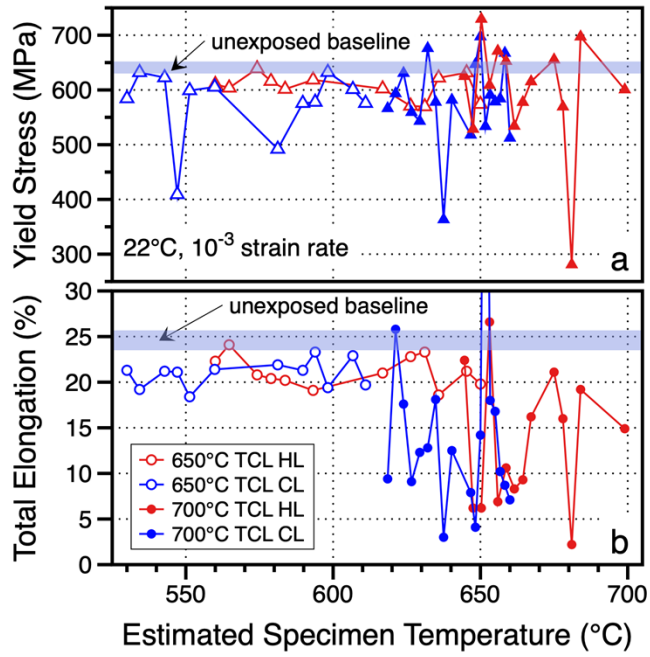

Figure 6. Post-exposure room-temperature tensile properties of APMT specimens as a function of estimated exposure temperature (a) yield stress and (b) total elongation. The open symbols are from the 650°C TCL and the closed symbols from the 700°C TCL. The baseline (as-received) properties are shown as a shaded band in each case.